ELSEVIER

Thermochimica Acta 338 (1999) 103–112

thermochimica acta

www.elsevier.com/locate/tca

Kinetic study of the isothermal and non-isothermal chlorination of a scheelite–wolframite concentrate with chlorine and sulphur dioxide[1]

C.J. Menéndez[a,b], E.L. Tavani[b,*], E.J. Nolasco[a]

[a]*Instituto de Investigaciones en Tecnología Química (INTEQUI), Universidad Nacional de San Luis, C.C. 290, 5700 San Luis, Argentina*

[b]*Centro de Tecnología de Recursos Minerales y Cerámica (CETMIC), Comisión de Investigaciones Científicas de la Provincia de Buenos Aires, C.C. 49, 1897 M.B. Gonnet, Argentina*

Received 10 February 1999; accepted 25 June 1999

Abstract

The isothermal and non-isothermal chlorination of a scheelite–wolframite concentrate with chlorine and sulphur dioxide was studied. Tests were made in a vertical reactor with a static bed and upward flow of reactive gases. The behaviour of the chlorination was analyzed from the identification of the volatile and non-volatile reaction products obtained in each case. The main identified reaction products were WO_2Cl_2, $FeCl_2$, $FeCl_3$, S_2, FeS, $CaSO_4$ and $CaCl_2$. Taking into account the most important physicochemical characteristics of the system, an empirical methodology to make chlorinations was proposed. The validity of the empirical methodology that we used was demonstrated utilizing data obtained under isothermal and non-isothermal conditions. Experimental results showed that the presence of non-volatile reaction products affects the chlorination under isothermal and non-isothermal conditions. A same kinetic dependence was found with both methods. Finally, the apparent activation energy and the rate constant of the reaction were determined through isothermal and non-isothermal methods. © 1999 Published by Elsevier Science B.V. All rights reserved.

Keywords: Kinetics; Isothermal; Non-isothermal; Chlorination; Scheelite; Wolframite

1. Introduction

The main kinetic aspects of the chemical reactions may be determined, in an alternating way, by means of isothermal and non-isothermal methods. In the isothermal method, the measurement of the conversion degree is performed as a function of time at constant reaction temperature. In the non-isothermal method, the measurement of the conversion degree is carried out when the sample is exposed to a systematic and controlled variation of the reaction temperature [1].

The non-isothermal method may give information about a process that is equivalent to the information obtained from the isothermal method. Acceptable results may be achieved with both methods when thermal decomposition reactions are studied. Nevertheless, the results obtained with the isothermal method and with the non-isothermal method do not show a reasonable agreement for more complex reactions. Several works were performed to establish the

[1]Presented in part at the 5th Southern Hemisphere Meeting on Mineral Technology, Buenos Aires, Argentina, May 8, 1997.

*Corresponding author. Fax: +54-221-4710075.

0040-6031/99/$ – see front matter © 1999 Published by Elsevier Science B.V. All rights reserved.
PII: S0040-6031(99)00204-X

advantages, difficulties and limitations of both methods [2–12].

Most of the metallic elements found in nature are combined with oxygen, while very few metallic elements are combined with chlorine [13]. Those metallic elements which have a large affinity with oxygen are called reactive metals. Reactive metal oxides have very high melting temperatures, they are stable and it is difficult to find a reducing agent adequate for the elimination of the combined oxygen. Whereas, the chlorides of these same metals have very low melting temperatures and they are highly volatile. This behaviour difference was used in processes of extractive metallurgy to recover some reactive metals. Thus, titanium, silicon, germanium and tantalium may be obtained from their corresponding chlorides [14,15].

The chlorination permits to replace the combined oxygen by chlorine through a gas–solid reaction [14,15]. The reaction starts with adsorption of chlorine on the surface of the reactive solid [16]. Then, the exchange of lattice oxygen by chlorine and the respective desorption of oxygen into the gaseous phase is produced. An electron transference occurs during the lattice oxygen conversion to molecular oxygen and during the Cl^{-1} formation. This electron transference was explained from the donor character of lattice oxygen atoms placed on the boundaries and dislocations of reactive crystallites [17].

Scheelite ($CaWO_4$) and wolframite ($Fe_xMn_{1-x}WO_4$) are the main tungsten-bearing minerals [13]. In our country, the larger known resources of tungsten with practical importance are the scheelite–wolframite concentrates. These concentrates are formed by associations of scheelite and of wolframite with different ratios of each mineral. The associations are difficult to be separated under favourable economic conditions. The presence of pyrite (FeS_2) was determined in several scheelite–wolframite concentrates. Whereas, scheelite and wolframite without association are found in insufficient amounts to be used on an industrial scale [18].

The chlorination is a process that permits the tungsten recovery from scheelite, wolframite and scheelite–wolframite concentrates. The recovery of the metallic element is performed from volatile tungsten oxychloride (WO_2Cl_2) obtained in each case [19]. The efficiency of the chlorination may be improved if a reducing agent is used to combine with the oxygen released during the chemical reaction. The sulphur dioxide showed a reducing behaviour acceptable with the mentioned minerals [20,21].

The chlorination of a scheelite–wolframite concentrate leads to the formation of volatile and non-volatile reaction products [21]. Non-volatile reaction products are deposited on the solid that did not react and the reactive gases must diffuse through this barrier to reach the reaction interface. In practice, it must be accepted that the interface is a zone of finite thickness extending for a small number of lattice units on the solid–gas contact surface [1].

The desorption of those products that are volatile is produced at the same time as the reaction occurs. Then, volatile products must diffuse in opposite directions with respect to reactive gases. This multiple diffusion during chlorination constitutes an important difference with respect to thermal decomposition reactions. In these systems, taking into account the reactant nature, the only diffusion that occurs is the one of the volatile products from the reaction interface.

The gas–solid heterogeneous reactions have a widely-known use in extractive metallurgy [14,22]. The chlorination is a particular case of these heterogeneous reactions. The kinetic analysis of the chlorination under isothermal and non-isothermal conditions is interesting since it would help to clarify aspects that do not occur in thermal decomposition reactions.

Accordingly, the aim of this work was to study the main kinetic aspects of the isothermal and non-isothermal chlorination of a scheelite–wolframite concentrate with chlorine and sulphur dioxide.

2. Experimental

The chlorination equipment used was composed of a vertical reactor with a static bed, a premixing chamber of gases at the bottom of the reactor, and three containers (one each for chlorine, sulphur dioxide and nitrogen) with their corresponding control valves and flowmeters. Into the reactor, the concentrate was placed on a ceramic fiber (kaowool). This fiber permitted the temperature homogenization and the distribution of the gaseous flow (inert gas and reactive gases). In each test 3 g of sample were used.

The thickness of the resulting bed did not present resistance to the diffusion of reactive gases.

The heating was made by an electric furnace with temperature control. The working temperature was reached by heating the reactor while inert gas circulated. When the system was stabilized at the working temperature, the inert gas was replaced by equal volume of reactive gases. As soon as the reaction time elapsed, the furnace was turned off and cooled down to room temperature while inert gas circulated again.

Fluidization and formation of channels in the bed occurred when a gas flow rate of 1000 ml min^{-1} was employed. Both difficulties were negligible at a flow rate of 500 ml min^{-1}. This flow rate of chlorine during 5 min represents near five times the amount required by the reaction stoichiometry. Then, the use of a chlorine flow rate of 300 ml min^{-1} allowed us to assure a reactive excess sufficient to finish the reaction studied. The flow was completed with 200 ml min^{-1} of sulphur dioxide employed as reducing agent in this work.

The excess of reactive gases, which remained without reacting at the exit of the reactor, was bubbled in an alkaline concentrate solution.

The sample of tungsten-bearing minerals that we used was collected in San Martín, San Luis, Argentina. The original sample was milled and enriched by gravity separation. Table 1 shows the chemical analysis of the scheelite–wolframite concentrate obtained by gravity separation. Gravity separation of the original sample was carried out with a jig and with a shaking table.

The mineral species found in the concentrate were scheelite (50–60% w/w), wolframite (25–35% w/w), pyrite (7–14% w/w), quartz (2–5% w/w) and feldspars (2–5% w/w). 90% of the concentrate had a particle size between 180 and 300 μm.

Table 1
Chemical analysis of the scheelite–wolframite concentrate obtained by gravity separation

	(% w/w)
WO_3	65.73
FeO	12.55
CaO	10.48
MnO	0.79
SiO_2	3.70
Al_2O_3	0.86
Na_2O	0.46
K_2O	0.12
S	2.42
LOI (1373 K)	3.10

The BET specific surface area of the concentrate was 0.4–0.5 $m^2\ g^{-1}$. The presence of close pores was not detected in any of the cases. Measurements of the BET specific surface area were performed with a Micromeritics Accusorb instrument by nitrogen adsorption.

Analyses by X-ray diffraction (XRD) were carried out using a Philips PW 1140/00 equipment, with a rotating sample holder and Cu Kα radiation. Morphologies were examined by scanning electron microscopy (SEM) with a JEOL JSM-T100 equipment. The surface chemical composition was determined by means of EDAX energy dispersive X-ray analysis (EDX) on a Philips 505 SEM.

Chemical analyses were made by titration and gravimetry for the major elements and by atomic absorption/emission (AA/AE) for the minor elements. AA/AE analyses were carried out with a Jarell Ash instrument. Tungsten extractions (α) corresponding to each experience were determined by chemical analysis of the unreacted samples (residues).

The kinetic analysis of the reaction under isothermal conditions was made at 1023, 1048 and 1073 K. The α values were determined for each of the selected temperatures as a function of time and at constant flow rates of the reactive gases (300 ml min^{-1} of chlorine + 200 ml min^{-1} of sulphur dioxide). Fig. 1 shows curves obtained for the isothermal chlorination of the scheelite–wolframite concentrate.

The kinetic analysis of the reaction under non-isothermal conditions was carried out between 773–1173 K. The α values were determined as a function of the temperature for a constant length of time (5 min) and at constant flow rates of the reactive gases (300 ml min^{-1} of chlorine + 200 ml min^{-1} of sulphur dioxide). Fig. 2 shows the curve obtained for the non-isothermal chlorination of the scheelite–wolframite concentrate.

3. Results and discussion

The volatile reaction products (which condensed at the reactor exit) and the non-volatile reaction products (deposited on the unreacted concentrate) formed dur-

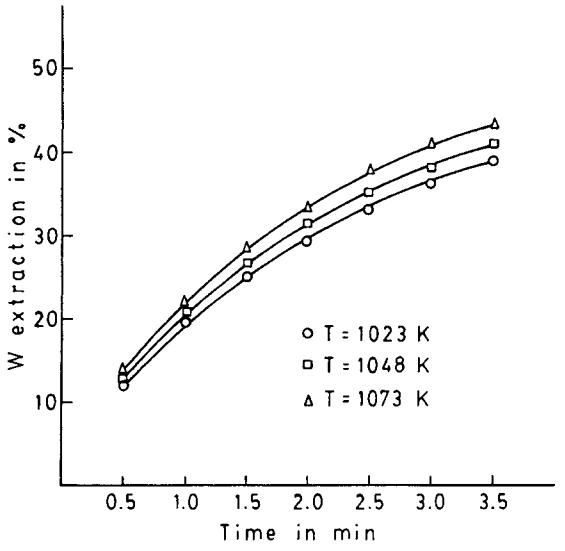

Fig. 1. Tungsten extraction versus time curves for the isothermal chlorination of the scheelite–wolframite concentrate.

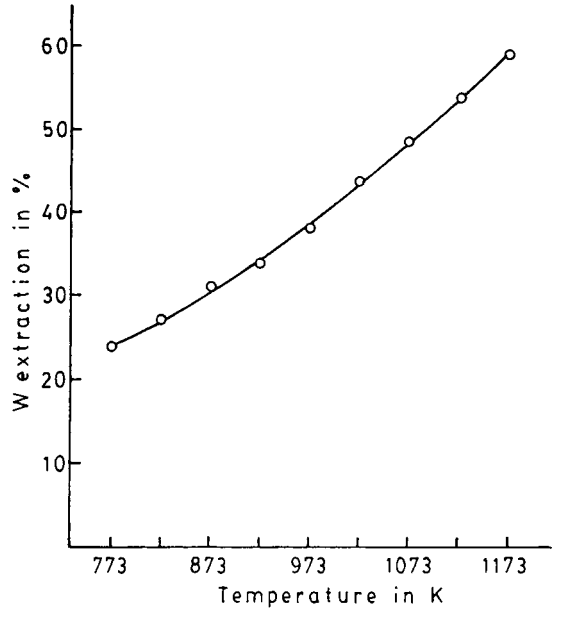

Fig. 2. Tungsten extraction versus temperature curve for the non-isothermal chlorination of the scheelite–wolframite concentrate.

ing chlorination were identified by XRD, SEM, EDX and chemical analysis. The reaction products identified were WO_2Cl_2 (volatile), $FeCl_2$ (volatile), $FeCl_3$ (volatile), S_2 (volatile), FeS (non-volatile), $CaSO_4$ (non-volatile) and $CaCl_2$ (non-volatile).

The WO_2Cl_2 formation occurred by chlorination of scheelite ($CaWO_4$) as well as of wolframite ($Fe_xMn_{1-x}WO_4$). Diffractograms of residues showed that wolframite disappeared (reacted) faster than scheelite. This behaviour was analyzed through the way in which the oxygen atoms were combined in scheelite (tetrahedral coordination: WO_4) and in wolframite (octahedral coordination: WO_6).

In WO_4, the four oxygen atoms complete their orbitals with six electrons from the tungsten (ionic bonds) and two electrons from calcium (ionic bonds). In WO_6, the six oxygen atoms complete their orbitals with six electrons from tungsten (ionic bonds) and electrons shared among them (covalent bonds). In both structures, the amount of electrons transferred by tungsten is the same.

In a chemical reaction, electrons transferred are the most labile ones (ionic). The WO_2Cl_2 formation from scheelite and from wolframite required removal of an equal amount of oxygen. However, the formation of each oxygen molecule (O_2) would be produced with a smaller transference of electrons from wolframite (two) than from scheelite (four). This minor transference of electrons would explain the higher reaction rate of wolframite with respect to scheelite.

The $FeCl_3$ formation was interpreted by means of two possible and different reaction sequences. The iron of pyrite and of wolframite at the beginning of the reaction was as divalent. The chlorination of both minerals led to $FeCl_2$ formation. Then, the $FeCl_2$ was transformed to $FeCl_3$ by chlorine [23]. Meanwhile, the oxygen released during the reaction contributed to the oxidation of iron (II) still unreacted. The chlorination continuation, in presence of iron (III) coming from the partial iron (II) oxidation, was an alternative way to obtain $FeCl_3$.

The thermal decomposition of pyrite, in inert atmosphere, leads to the formation of sulphur (S_2) and pyrrhotite (FeS). At temperatures near 973 K, transformations higher than 60% were reached in periods of time <20 min. The rate of this transformation depends on the temperature and particle size of the mineral [24,25]. In our case, the pyrrhotite and sulphur were identified after heating the concentrate in the reactor while an inert gas flow circulated. This situation changed when the inert gas was replaced by

reactive gases (Cl_2 + SO_2). The oxygen released during chlorination reacts with SO_2 to form $CaSO_4$ and with pyrite (still without thermal transformation) and pyrrhotite to form $CaSO_4$ and iron oxides. To confirm the pyrite participation in the reaction, chlorinations without sulphur dioxide were made. Concentrates with different pyrite contents were used in these tests. The $CaSO_4$ presence was determined in those residues coming from concentrates with a pyrite content higher than 14%.

The $CaCl_2$ is the non-volatile reaction product with lower melting temperature. The salt melts at 1055 K and in liquid state flows, by gravity, towards the ceramic fiber. The presence of the molten salt in the ceramic fiber impedes an efficient distribution of the gaseous flow through the bed. By thermodynamic analysis, it was determined that $CaSO_4$ is easily formed than $CaCl_2$ [26]. The $CaSO_4$ formation was favored when chlorination was performed in presence of a high pyrite content [21]. According to pyrite content of the concentrate and to the amount of sulphur dioxide that we used, $CaCl_2$ formation was negligible.

The occurrence of a thermal gradient that decreased while the test temperature increased was determined in all isothermal and non-isothermal chlorinations performed in this work. The chlorination temperature reached a maximum between 0.5–1.5 min and then decreased. After 2–3 min the temperature was stabilized in its initial value. Residues obtained in these conditions did not have sulphur-bearing minerals.

The occurrence of the thermal gradient was explained from the exothermic nature of pyrite oxidation [14]. At temperatures lower than 873 K, the pyrite and the oxygen released during the chlorination may react according to

$$4FeS_2\ (s) + 11O_2\ (g) \rightarrow 2Fe_2O_3\ (s) + 8SO_2\ (g) \quad (1)$$

At temperatures higher than 973 K, the thermal decomposition of pyrite occurred by a reaction such as

$$2FeS_2\ (s) \rightarrow 2FeS\ (s) + S_2\ (g) \quad (2)$$

The volatilization of S_2 (condensed at the reactor exit) changed the sulphur content of the concentrate that may react with the oxygen released during the chlorination. Then, the thermal gradient observed at temperatures higher than 973 K was lower that those determined at 773 and 873 K.

A partial sintering of the residue was determined in those tests with higher thermal gradient. This sintering changed the porosity of the static bed and impeded an efficient contact between the reactive gases and the concentrate. In order to favor the thermal decomposition of the pyrite and so minimize the occurrence of the thermal gradient, isothermal chlorinations were carried out at 1023, 1048 and 1073 K.

The methodology used under isothermal and non-isothermal conditions was modified taking into account the temperature fall due to the exhaustion of pyrite. To compensate this situation, the temperature of the electric furnace that heated the reactor was increased once the reaction started. The average of the maximum temperature and the final temperature was taken as the test temperature. The results were considered as acceptable when the differences of both values (maximum and final) were lower than 7 K.

The heterogeneity of reaction products (volatile and non-volatile) impeded the determination of conversion degree by weight loss. Therefore, the α values were determined through a destructive chemical analysis using a new sample for each test. The α values that had an unsuitable reproduction ($>\pm 3\%$) were rejected and the corresponding tests were repeated under the same operative conditions. Each α value reported in this paper was the average of two chlorinations performed in the same way with a similar reproduction. The lack of reproduction of the results obtained was attributed to the formation of channels, sintering and other operational problems typical of small reactors with a static bed.

The kinetic analysis of the isothermal chlorination (Fig. 1) was performed from the general rate equation

$$g(\alpha) = kt \quad (3)$$

where $g(\alpha)$ is the proposed rate equation, α is the tungsten extraction after time t at constant temperature and k is the rate constant of the process. The $g(\alpha)$ that describes the α versus t curve was selected from Eq. (3). The possible selected forms of $g(\alpha)$ are given in Table 2 [1]. The $g(\alpha)$ versus t plot is a straight line if the selection of $g(\alpha)$ is correct. The slope of this straight line is equal to k. The linearity of each $g(\alpha)$ versus t plot was evaluated by the least square method.

Table 2
Rate equations examined in the kinetic analysis

Mechanism	$g(\alpha)$	Symbol
One-dimensional diffusion	α^2	D1
Two-dimensional diffusion	$(1-\alpha)\ln(1-\alpha)+\alpha$	D2
Three-dimensional diffusion		
Jander equation	$(1-(1-\alpha)^{1/3})^2$	D3
Three-dimensional diffusion		
Ginstling–Brounshtein equation	$(1-2\alpha/3)-(1-\alpha)^{2/3}$	D4
Phase boundary controlled reaction		
contracting area	$1-(1-\alpha)^{1/2}$	R2
contracting volume	$1-(1-\alpha)^{1/3}$	R3
Unimolecular decay law	$-\ln(1-\alpha)$	F1
Random nucleation and growth of nuclei		
Avrami–Erofeev equation	$(-\ln(1-\alpha))^{1/2}$	A2
Avrami–Erofeev equation	$(-\ln(1-\alpha))^{1/3}$	A3
Avrami–Erofeev equation	$(-\ln(1-\alpha))^{1/4}$	A4

Table 3
Rate constants and linear regression coefficients calculated from isothermal data

T (K)	k (min^{-1})	r
1023	0.007048	0.9993
1048	0.007986	0.9994
1073	0.009217	0.9979

The best agreement found for the isothermal chlorination of the scheelite–wolframite concentrate was given by a rate equation ($g(\alpha)=(1-(1-\alpha)^{1/3})^2$) based on a diffusion mechanism with spherical symmetry (D3). This three-dimensional diffusion process, through the layer of reaction products, was the controlling stage of the total kinetics. Table 3 shows the calculated values of the rate constant and corresponding linear regression coefficients.

The rate constant is related with the temperature (T) by the Arrhenius equation

$$k = A\mathrm{e}^{-E/RT} \tag{4}$$

where E is the apparent activation energy, R the gas constant and A is often referred as frequency factor. The E value is affected by the experimental conditions used, including the weight, size, impurity contents, compaction and crystallinity of the sample, etc. The A factor, in homogeneous reactions, represents the frequency of effective collisions between reacting molecules. Its physical meaning is not well defined in heterogeneous reactions. The linear form of the Arrhenius equation (Fig. 3) permits to calculate A and E from the $\ln k$ versus $1/T$ plot. Table 4 shows the obtained values and the corresponding linear regression coefficient.

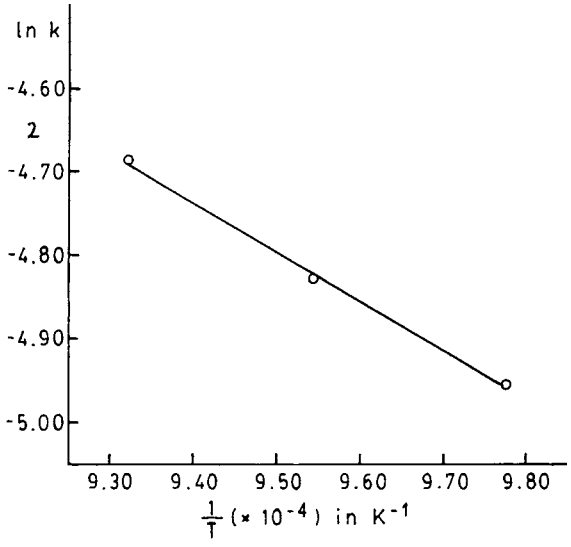

Fig. 3. Arrhenius plot for k values calculated from isothermal chlorinations performed at 1023, 1048 and 1073 K.

Table 4
Kinetic parameters calculated from isothermal data

Parameters	
E (kJ mol^{-1})	46.9
A (min^{-1})	1.74
r	0.9985

The methodology used in the kinetic analysis of non-isothermal thermal decomposition reactions involves a simultaneous change of reaction temperature and time (dependent variables). Both variables may be related among them by the heating rate. According to the heating rates used in mentioned works (5–10 K min^{-1}), long reaction times are required to finish the study. Then, reaction times of tests performed under non-isothermal conditions are longer than reaction times of tests carried out under isothermal conditions. In this work, it was considered the possibility to change the reaction temperature in a discontinuous and controlled manner (systematic) while the other operative variables were constant.

In order to determine the adequate length of time, chlorinations at 923, 1023 and 1123 K were performed during periods of time longer than the ones indicated in Fig. 1. After 5 min, the α values showed little changes. According to these results, the non-isothermal chlorinations were performed at 773, 823, 873, 923, 973, 1023, 1073, 1123 and 1173 K with flow rates of 300 ml min^{-1} for chlorine and 200 ml min^{-1} for sulphur dioxide and at a constant time of 5 min.

The use of a new sample for each chlorination and the discontinuous variation of temperature were changes made to the methodology used in thermal decomposition reactions. In these decomposition reactions, the conversion degree is determined by weight loss (non-destructive test) and the reaction temperature and time change simultaneously with each α value determined.

The kinetic analysis of the non-isothermal chlorination (Fig. 2) was carried out by means of the integration method using a characteristic temperature (Tc) to evaluate the temperature integral [1,3,27–29]. The integral evaluation is easier by performing several approximations. One of these approximations requires an adequate selection of Tc so that the measured temperature (T) may fulfill with the inequality $|T-\mathrm{Tc}|<<\mathrm{Tc}$. Taking logarithms and rearranging terms it is possible to obtain an equation whose simplified expression is

$$\ln g(\alpha) = \ln g(\alpha c) + (E/R\mathrm{Tc}^2)(T-\mathrm{Tc}) \qquad (5)$$

where $g(\alpha)$ are the same rate equations used in the isothermal method. The $\ln g(\alpha)$ versus $(T - \mathrm{Tc})$ plot is a straight line if the selection of $g(\alpha)$ is correct.

The Tc value changes with the nature of the reaction to be evaluated. Thus, when all the reaction products are volatile (as in the pyrolisis of polymers), Tc is defined as the temperature at which $1 - 1/\alpha = 1/e$, where $e = 2.71828$. For reactions in which the weight loss is a fraction of the total weight (as in the pyrolisis of hydrated salts), a method generally used is to choose Tc where $d\alpha/dT$ is maximum. In both systems, reactions start and are finished within a temperature narrow range, the Tc value is defined from other variables and the temperature inequality is easy to be fulfilled.

In those systems with change of reactant concentrations, reaction products are heterogeneous and phase transformations occur within a temperature wide range, the Tc definition is not so easy as in previous cases. The average of the initial temperature and final temperature is a value that may be used to obtain an acceptable approximation of the temperature inequality.

The best agreement found for the non-isothermal chlorination of the scheelite–wolframite concentrate corresponded to the same rate equation ($g(\alpha) = (1 - (1 - \alpha)^{1/3})^2$) determined under isothermal conditions. The E was calculated from the ($E/R\,\mathrm{Tc}^2$) slope corresponding to the $\ln g(\alpha)$ versus $(T - \mathrm{Tc})$ plot. As in the previous case, the linearity of each plot was evaluated by the least square method. Table 5 shows the E and r values calculated from the non-isothermal chlorinations performed between 773 and 1173 K.

The validity of results achieved depends on that k does not change its form with the temperature [9]. This behaviour may be determined from the slope corresponding to the relationship between $\ln k$ and $1/T$ (Arrhenius equation). Assuming that $g(\alpha)$ versus t plots had an acceptable linearity in all tests made between 773–1173 K, the possibility to estimate the k value from Eq. (3) and the α value obtained at 5 min for each temperature was considered.

The values so obtained had a 10% difference with respect to those determined from isothermal data (923,

Table 5
Apparent activation energies calculated from non-isothermal data (ΔT = 773–1173 K and ΔT = 823–1173 K)

Parameters	773–1173 K	823–1173 K
E (kJ mol^{-1})	43.2	45.4
r	0.9992	0.9989

1023, 1048, 1073 and 1123 K). The $g(\alpha) = (1 - (1 - \alpha)^{1/3})^2$ versus t plots for these isothermal chlorinations showed a good linearity between 0.5 and 5.0 min. The $g(\alpha)$ values at 0.5 min were negligible with respect to $g(\alpha)$ values at 5.0 min and the extension of the straight lines that joined both points intercepted the time axis between 0.4 and 0.5 min. Then, each $g(\alpha)$ value was divided by 4.5 min instead of 5.0 min which allowed us to perform k estimations that had a reasonable agreement ($\leq$2.5%) with the values obtained from isothermal data.

The linear regression coefficient of the ln k versus $1/T$ plot for k values estimated between 773 and 1173 K was 0.9921 and the major dispersion of the lnk occurred at $1/T = 12.937 \times 10^{-4}\ K^{-1}$ (773 K). The exclusion of this value improved the plot linearity ($r = 0.9942$). Fig. 4 shows the ln k versus $1/T$ plot (dark line) for k values estimated between $1/T = 8.525 \times 10^{-4}$ (1173 K) and $12.151 \times 10^{-4}\ K^{-1}$ (823 K), the k value estimated from the tungsten extraction obtained at 773 K (dark line) and the k value that would correspond if the indicated behaviour between 8.525×10^{-4} and $12.151 \times 10^{-4}\ K^{-1}$ is maintained (ideal behaviour) up to $12.937 \times 10^{-4}\ K^{-1}$ (dotted line). According to k values illustrated

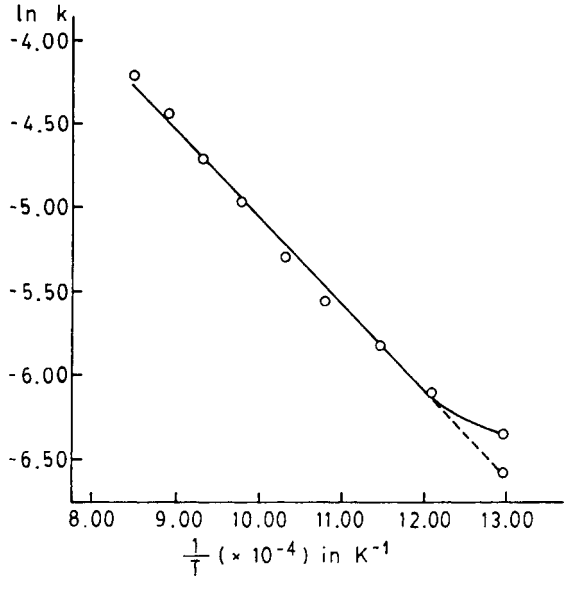

Fig. 4. Arrhenius plot for k values estimated from non-isothermal chlorinations performed between 823 and 1173 K. At $1/T = 12.937\ 10^{-4}\ K^{-1}$ (T = 773 K), the k value estimated from the experimental datum (—) and the k value ideal (- - -) are also illustrated.

at $1/T = 12.937 \times 10^{-4}\ K^{-1}$, the tungsten extraction obtained in the mentioned point was higher than that expected from ideal behaviour. This fact was analyzed from the calcium sulphate formation and the pyrite presence in the concentrate.

The calcium sulphate was obtained by chlorination of scheelite ($CaWO_4$ (s) + Cl_2 (g) + SO_2 (g) $\leftrightarrow$ WO_2Cl_2 (g) + $CaSO_4$ (s)). The salt was deposited on the unreacted concentrate and its formation increased with temperature. The tungsten extraction was expressed as a ratio of its initial content in the concentrate (w/w) while the residue weight of each test was taken as reference to express the salt amount formed (w/w).

Results of tests performed at 773 K (it did not fulfill the Arrhenius equation) and at 823 K (it fulfilled the Arrhenius equation) are shown to compare them. At 773 K, the tungsten extraction was 0.24 w/w, the weight residue 2.1 g and the amount of calcium sulphate formed 0.03 w/w. The higher tungsten dissolution with respect to the salt formed was produced because more than half of the tungsten extracted came from wolframite dissolution and this mineral does not participate in calcium sulphate formation. At 823 K, the tungsten extraction was 0.27 w/w, the residue weight 1.9 g and the salt amount formed 0.04 w/w. The texture and the surface chemical composition of both residues were similar (SEM-EDX).

In our system, the total kinetics was controlled by the diffusion process through calcium sulphate. At the same time, the diffusion process depended on layer thickness of salt formed and its corresponding texture. Both characteristics were similar in the residues obtained at 773 and 823 K. Then, the behaviour change shown in Fig. 4 would not be originated in the calcium sulphate formation.

The pyrite and the sulphur dioxide were combined with the released oxygen during chlorination. An efficient removal of this oxygen led to a high yield of the reaction [20,21]. The combination of pyrite with oxygen occurred at low temperature in a proportion higher than with sulphur dioxide. This fact was determined by means of the Gibbs free energy [21]. On the other hand, as it was above mentioned, the pyrite thermal decomposition was low at 773 K. Then, the higher tungsten extraction at 773 K would be produced from a secondary reaction and not by a change in the chlorination reaction mechanism. The kinetic

analysis performed between 823 and 1173 K (Table 5) confirmed this behaviour. Results obtained showed that the reaction mechanism remained and that a minimum change of apparent activation energy was produced.

4. Conclusions

The main phase transformations occurring in the isothermal and non-isothermal chlorination of the scheelite–wolframite concentrate with chlorine and sulphur dioxide were established from volatile and non-volatile reaction products formed in each case.

An empirical methodology that takes into account the physicochemical characteristics of the system was proposed to make chlorinations under isothermal and non-isothermal conditions.

The occurrence of a thermal gradient that decreased with the exhaustion of the pyrite contained in the concentrate was determined in isothermal and non-isothermal chlorinations performed in this work. The temperature of the electric furnace that heated the reactor was modified adequately to compensate this situation. The measurements of the tungsten extractions (isothermal and non-isothermal methods) were carried out by chemical analysis using a new sample for each test. In the non-isothermal method, the reaction temperature was changed in a discontinuous and controlled manner while the other variables were constant.

The main kinetic aspects (mechanism and parameters) of the reaction were analyzed from data obtained under isothermal and non-isothermal conditions. A same rate equation, based on a diffusion mechanism with spherical symmetry, was determined with both methods. The control of the total kinetics corresponded to a diffusion process through the reaction products deposited on the unreacted concentrate.

In the non-isothermal method, the kinetic aspects were analyzed from a single tungsten extraction versus temperature curve. At the same time, rate constants were estimated assuming that $g(\alpha)$ versus t plots had an acceptable linearity and the behaviour of these constants with the temperature was evaluated through the Arrhenius equation.

The value of the apparent activation energy and rate constants estimated from the non-isothermal data were consistent with respect to those determined from isothermal data, despite the approximation adopted in the empirical methodology that we used.

References

[1] C.H. Bamford, C.F.H. Tipper, Comprehensive Chemical Kinetics, Elsevier, Amsterdam, 1980.
[2] F.J. Gotor, M. Macías, A. Ortega, J.M. Criado, Int. J. Chem. Kinet. 30 (1998) 647.
[3] C. Popescu, E. Segal, Int. J. Chem. Kinet. 30 (1998) 313.
[4] Z. Brito, V. Torrealba, G. Sánchez, L. Hernández, Lat. Am. Appl. Res. 26S (1996) 31.
[5] A. Ersoy-Meriçboyu, S. Küçükbayrak, R. Yavuz, Thermochim. Acta 223 (1993) 121.
[6] Zhao Yu-Ting, Zhang Jian-Hua, Sun Tong-Shan, Yang Zhao-He, Thermochim. Acta 223 (1993) 101.
[7] N.S. Felix, B.S. Girgis, J. Thermal Anal. 35 (1989) 743.
[8] A.M. El-Awad, R.M. Mahfouz, J. Thermal Anal. 35 (1989) 1413.
[9] E. Urbanovici, E. Segal, Termochim. Acta 111 (1987) 335.
[10] J.M. Criado, A. Ortega, C. Real, React. Solids 4 (1987) 93.
[11] C. Santiago, A. Arnaiz, T. Guaraya, L. Lorente, J.M. Arrieta, React. Solids 2 (1986) 163.
[12] A.W. Coats, J.P. Redfern, Nature 201 (1964) 68.
[13] W.H. Blackburn, W.H. Dennen, Principles of Mineralogy, Wm. C. Brown Publishers, Dubuque, 1994.
[14] T. Rosenqvist, Fundamentos de Metalurgia Extractiva, Editorial Limusa, México, 1987.
[15] Z. Szczygiel, A. Torres, Metalurgia no Ferrosa, Editorial Limusa, México, 1984.
[16] F. Réti, I. Bertóti, G. Mink, T. Székely, React. Solids 3 (1987) 329.
[17] J. Andrade Gamboa, D.M. Pasquevich, J. Am. Ceram. Soc. 75 (1992) 2934.
[18] V. Angelelli, Yacimientos Metalíferos de la República Argentina, Comisión de Investigaciones Científicas de la Provincia de Buenos Aires, La Plata, 1984.
[19] S.W.H. Yih, C.T. Wang, Tungsten: Sources, Metallurgy, Properties and Applications, Plenum Press, New York, 1979.
[20] C.J. Menéndez, E.J. Nolasco, E.L. Tavani, E. Pereira, Mater. Chem. Phys. 40 (1995) 273.
[21] C.J. Menéndez, E.J. Nolasco, E.L. Tavani, E. Pereira, Can. Metall. Quart. 37 (1998) 379.
[22] H.Y. Soh, M.E. Wadsworth, Cinética de los Procesos de la Metalurgia Extractiva, Editorial Trillas, México, 1986.
[23] K. Nagata, P. Bolsaitis, Int. J. Miner. Process. 19 (1987) 157.
[24] J. Oberholzer, M.A. Luengos, J.J. Andrade G., A.E. Bohé, D.M. Pasquevich, Proc. IV International Conference on Clean Technologies for the Mining Industry, 2 (1998) 867.

[25] Dj. Jovanovic, J. Thermal Anal. 35 (1989) 1483.
[26] B.N. Chakravarti, A.T. Prince, Proc. Third Annual Conference of Reactive Metals, American Institute of Mining, Metallurgical and Petroleum Engineering, Buffalo, NY, 2 (1959) 349.
[27] E.F. Aglietti, H.J. Gasalla, J.M. Porto López, Lat. Am. Appl. Res. 18 (1988) 43.
[28] P. Vallet, Thermogravimétrie, Gauthier-Villars, Paris, 1972.
[29] H.H. Horowitz, G. Metzger, Analyt. Chem. 35 (1963) 1464.